Title

Actin-based motility allows Listeria monocytogenes to avoid autophagy in the macrophage cytosol

Journal

Cellular Microbiology, 20(9)

ISSN

1462-5814

Authors

Cheng, Mandy I
Chen, Chen
Engström, Patrik
et al.

Publication Date

2018-09-01

DOI

10.1111/cmi.12854

Peer reviewed

Received: 21 November 2017 | Revised: 3 April 2018 | Accepted: 23 April 2018

DOI: 10.1111/cmi.12854

RESEARCH ARTICLE

WILEY

Actin-based motility allows *Listeria monocytogenes* to avoid autophagy in the macrophage cytosol

Mandy I. Cheng[1] | Chen Chen[1] | Patrik Engström[1] | Daniel A. Portnoy[1,2] | Gabriel Mitchell[1]

[1] Department of Molecular and Cell Biology, University of California, Berkeley, CA, USA

[2] School of Public Health, University of California, Berkeley, CA, USA

Correspondence
Gabriel Mitchell, Department of Molecular and Cell Biology, University of California, Berkeley, CA 94720, USA.
Email: gabriel.mitchell@berkeley.edu

Funding information
National Institutes of Health, Grant/Award Numbers: 1R01 AI027655 and 1P01 AI063302; Sweden-America Foundation; Svenska Sällskapet för Medicinsk Forskning; Stiftelsen Olle Engkvist Byggmästare; Natural Sciences and Engineering Research Council of Canada; Fonds de recherche du Québec - Santé; Fonds de recherche du Québec - Nature et technologies; Defense Threat Reduction Agency, Grant/Award Number: HDTRA1-13-1-0003

Abstract

Listeria monocytogenes grows in the host cytosol and uses the surface protein ActA to promote actin polymerisation and mediate actin-based motility. ActA, along with two secreted bacterial phospholipases C, also mediates avoidance from autophagy, a degradative process that targets intracellular microbes. Although it is known that ActA prevents autophagic recognition of *L. monocytogenes* in epithelial cells by masking the bacterial surface with host factors, the relative roles of actin polymerisation and actin-based motility in autophagy avoidance are unclear in macrophages. Using pharmacological inhibition of actin polymerisation and a collection of *actA* mutants, we found that actin polymerisation prevented the colocalisation of *L. monocytogenes* with polyubiquitin, the autophagy receptor p62, and the autophagy protein LC3 during macrophage infection. In addition, the ability of *L. monocytogenes* to stimulate actin polymerisation promoted autophagy avoidance and growth in macrophages in the absence of phospholipases C. Time-lapse microscopy using green fluorescent protein-LC3 macrophages and a probe for filamentous actin showed that bacteria undergoing actin-based motility moved away from LC3-positive membranes. Collectively, these results suggested that although actin polymerisation protects the bacterial surface from autophagic recognition, actin-based motility allows escape of *L. monocytogenes* from autophagic membranes in the macrophage cytosol.

KEYWORDS

ActA, bacteria, PLCs, ubiquitin, xenophagy

1 | INTRODUCTION

Although macrophages have an impressive arsenal of antimicrobial processes, they are one of the primary cells targeted by many species of intracellular bacterial pathogens. Therefore, in order to survive within macrophages, bacteria utilise numerous strategies to avoid and manipulate cell-autonomous defences (Mitchell, Chen, & Portnoy, 2016). Although some intracellular bacterial pathogens employ secreted effectors to remodel the host cell and form an intravacuolar replicative niche derived from the endomembrane network, others escape and proliferate in the host cytosol. Most cytosolic bacterial pathogens exploit host actin polymerisation to move within and between host cells, a process for which the main function is assumed to be the dissemination of the pathogen within host tissues (Lamason & Welch, 2017). However, exploitation of the actin polymerisation machinery by cytosolic bacterial pathogens may impact other cellular processes, including host cell-autonomous defences such as autophagy (Mostowy & Shenoy, 2015).

Autophagy contributes to host cell homeostasis by targeting protein aggregates, dysfunctional organelles, and microbes for degradation in lysosomal-like compartments (Galluzzi et al., 2017). Processes that rely on the autophagy machinery constitute a multilayered network of autonomous defences that protect the endomembrane system and the host cytosol against invading microbes (Huang &

Brumell, 2014; Mitchell et al., 2018). For example, microbes that escape the endomembrane system and access the cytosol may be recognised and tagged by ubiquitin chains, which recruit autophagy receptors such as p62 (Huang & Brumell, 2014; Randow & Youle, 2014). In turn, these autophagy receptors function as molecular bridges that link microbes to LC3-positive autophagic membranes and promote autophagic engulfment. Numerous intracellular pathogens have evolved mechanisms to avoid or exploit autophagy as a strategy of pathogenesis (Huang & Brumell, 2014).

The Gram-positive bacterium *Listeria monocytogenes* is a foodborne pathogen that grows in a wide variety of host cells and constitutes a model organism to study host-pathogen interactions (Cossart, 2011). *L. monocytogenes* escapes the entry vacuole by secreting a pore-forming toxin listeriolysin O and two phospholipases C (PLCs; PlcA and PlcB; Schnupf & Portnoy, 2007; Smith et al., 1995). *L. monocytogenes* then replicates rapidly in the host cytosol and densely covers its surface with the bacterial protein ActA. ActA induces host actin polymerisation by acting as a nucleation promoting factor (Kocks et al., 1992; Pistor, Chakraborty, Niebuhr, Domann, & Wehland, 1994), which allows *L. monocytogenes* to perform actin-based motility and spread from cell-to-cell (Portnoy, Auerbuch, & Glomski, 2002; Tilney & Portnoy, 1989).

ActA has several functional domains that interact with the actin polymerisation machinery including an acidic stretch, an actin monomer-binding region, a cofilin homology sequence, and a central region with proline-rich repeats. Although the cofilin homology sequence is required for the activation of the Arp2/3 complex and plays a pivotal role in ActA function (Lauer, Theriot, Skoble, Welch, & Portnoy, 2001; Pistor et al., 2000), the other domains exert modest contributions to actin-based motility and cell-to-cell spread (Skoble, Auerbuch, Goley, Welch, & Portnoy, 2001; Skoble, Portnoy, & Welch, 2000; Smith, Theriot, & Portnoy, 1996). For example, the central region contains proline-rich repeats that control the rate and duration of actin-based motility by recruiting enable/vasodilator-stimulated phosphoprotein and profilin (Auerbuch, Loureiro, Gertler, Theriot, & Portnoy, 2003; Niebuhr et al., 1997; Smith, Theriot, & Portnoy, 1996). While single mutations within the actin monomer-binding region or the central region do not prevent actin-based motility, a double mutant in these regions strongly impairs the intracellular movement of *L. monocytogenes* (Skoble et al., 2001). Although the primary function of ActA is to mediate intracellular movement and cell-to-cell spread, ActA has also been implicated in bacterial aggregation and biofilm formation, internalisation in host cells, escape from the entry vacuole, induction of NF-κB, and autophagy avoidance (Pillich, Puri, & Chakraborty, 2017).

L. monocytogenes actively interferes with growth-restricting autophagy using PLCs and ActA (Mitchell et al., 2015; Mitchell et al., 2018). Results from previous studies demonstrated that ActA and PLCs primarily allow *L. monocytogenes* to interfere with autophagy during growth in the host cytosol (Mitchell et al., 2018; Tattoli et al., 2013). However, *L. monocytogenes* can also be targeted by autophagy while transitioning from a vacuole to the host cytosol (Lam, Cemma, Muise, Higgins, & Brumell, 2013; Meyer-Morse et al., 2010; Mitchell et al., 2018; Thurston, Wandel, von Muhlinen, Foeglein, & Randow, 2012). Although PLCs act on autophagic membranes and interfere with the sequestration of bacteria within autophagosomes (Mitchell et al., 2015; Mitchell et al., 2018; Tattoli et al., 2013), ActA prevents the formation of a ubiquitin coat on the bacterial surface and the subsequent recruitment of autophagy receptors (Mostowy et al., 2011; Perrin, Jiang, Birmingham, So, & Brumell, 2004; Yoshikawa et al., 2009).

The exact mechanism by which ActA prevents autophagy is still under debate. An early study by Perrin et al. (2004) suggested that the ability of *L. monocytogenes* to perform actin-based motility interferes with the formation of a ubiquitin coat on the bacterial surface during macrophage infection but did not establish a link between ubiquitylation and targeting by autophagy. A subsequent study by Yoshikawa et al. (2009) confirmed that ActA mediates autophagy avoidance by blocking the ubiquitylation of *L. monocytogenes* during infection of epithelial cells. However, in apparent contradiction with Perrin et al. (2004), this study showed that ActA interferes with ubiquitylation by coating and masking the bacterial surface with components of the host actin polymerisation machinery such as the Arp2/3 complex or enable/vasodilator-stimulated phosphoprotein. Importantly, results from Yoshikawa et al. (2009) suggested that the ability of ActA to prevent recognition of *L. monocytogenes* by autophagy is independent of actin polymerisation and actin-based motility. Although the conclusions of Yoshikawa et al. (2009) dominate the current literature (Choy & Roy, 2013; Gong, Devenish, & Prescott, 2012; Huang & Brumell, 2014; Kimmey & Stallings, 2016; Mostowy, 2013; Mostowy & Shenoy, 2015; Pareja & Colombo, 2013; Welch & Way, 2013), it is still unclear if actin polymerisation and actin-based motility play a role in the avoidance of *L. monocytogenes* from autophagy during macrophage infection.

In this study, we used bacterial genetics, immunofluorescence, and time-lapse microscopy to investigate the role of actin polymerisation and actin-based motility in the avoidance of *L. monocytogenes* from autophagy during macrophage infection. In agreement with Perrin et al. (2004), our results demonstrated that actin polymerisation and actin-based motility protect the bacterial surface from autophagic recognition and promote the escape of *L. monocytogenes* from autophagic membranes in the macrophage cytosol. Our results also demonstrated that, in absence of PLCs, the ability to polymerise actin is required for *L. monocytogenes* growth in macrophages.

2 | RESULTS

2.1 | Inhibition of actin polymerisation with cytochalasin D promotes ubiquitylation of *L. monocytogenes* and the recruitment of p62 during macrophage infection

L. monocytogenes mutants lacking ActA are polyubiquitylated (polyUb) and recruit the ubiquitin-binding autophagy receptor p62 during intracellular infection (Mostowy et al., 2011; Perrin et al., 2004; Yoshikawa et al., 2009). In order to evaluate the role of actin polymerisation in the avoidance of *L. monocytogenes* from autophagic recognition, the effect of the actin polymerisation inhibitor cytochalasin D on the colocalisation of *L. monocytogenes* with polyUb and p62 was monitored during infection of bone marrow-derived macrophages (BMMs). As previously reported, Δ*actA* bacteria colocalised with polyUb

(Figure 1a) and p62 (Figure 1b), and bacteria positive for polyUb were consistently positive for p62 (Figure 1c). Surprisingly, treatment of macrophages with cytochalasin D dramatically increased the colocalisation of wild-type (WT; 10403S) *L. monocytogenes* with polyUb and p62 (Figure 1a,b,d). Similar results were observed with another commonly used laboratory strain, EGD-e (Figure 1e; Becavin et al., 2014). These results suggested that actin polymerisation was important for *L. monocytogenes* to avoid colocalisation with polyUb and the autophagy receptor p62 during macrophage infection.

2.2 | ActA mutants colocalise with p62 and LC3 during macrophage infection

The hypothesis that *L. monocytogenes* uses actin polymerisation to interfere with autophagic recognition was further tested using ActA mutants that are either weakly (ActA$^{\Delta AS}$, ActA$^{\Delta AB}$, and ActA^{PR}) or strongly (ActA$^{\Delta AB;PR}$ and ActA^{CH}) impaired in their ability to polymerise actin and mediate actin-based motility (Lauer et al., 2001; Skoble et al., 2001; Figure 2a). Colocalisation of WT and the ActA mutants with filamentous actin (F-actin) and p62 was evaluated during macrophage infection. The presence of actin tails is indicative of bacteria undergoing actin-based motility and moving within the cell (Theriot, Mitchison, Tilney, & Portnoy, 1992). WT bacteria formed actin clouds and actin tails but rarely colocalised with p62 (Figure 2b). Interestingly, two types of p62$^+$ structures colocalised with ActA mutants, either distinct rod-shaped "bacteria-like" structures observed with the Δ*actA* strain or "punctae-like" structures closely associated with the bacterial surface (Figure 2c,d). Similarly to Δ*actA*, strongly impaired ActA mutants (ActA$^{\Delta AB;PR}$ and ActA^{CH}) rarely colocalised with F-actin but consistently colocalised with p62 in the shape of bacteria (Figure 2e,f). These results contrast with those obtained in different cell types (Yoshikawa et al., 2009), including mouse embryonic fibroblasts (MEFs; Figure S1), which suggested that ActA-mediated actin polymerisation interferes with autophagy in a subset of host cells (e.g., macrophages). Weakly impaired ActA mutants (ActA$^{\Delta AS}$, ActA$^{\Delta AB}$, and ActA^{PR}) had similar levels of actin cloud formation but exhibited significantly fewer actin tails in comparison with the WT strain (Figure 2e) and colocalised with punctae-like p62$^+$ structures (Figure 2d,f). Notably, the p62$^+$ punctae-like structures associated with bacteria that had formed actin clouds but usually localised to bacterial poles associated with a weaker actin signal (Figure 2d). Bacteria that formed actin tails rarely associated with p62 (<1%, 2 out of 202 actin tail$^+$ bacteria, 3 hr post-infection; Figure 2g). These results showed that *L. monocytogenes* undergoing actin-based motility did not associate with p62 and that defects in ActA-mediated actin polymerisation led to phenotypically distinct associations with p62.

In order to gain insight into the significance of the punctae-like and bacteria-shaped p62$^+$ structures, the kinetics of colocalisation of p62 with WT, the weakly impaired mutant ActA^{PR}, and the strongly impaired mutant ActA^{CH} were evaluated during macrophage infection (Figure 3). All strains associated transiently with punctae-like p62$^+$ structures early during infection, although this association lasted longer for the weakly impaired mutant ActA^{PR}. However, only the strongly impaired mutant (ActA^{CH}) was uniformly covered with p62

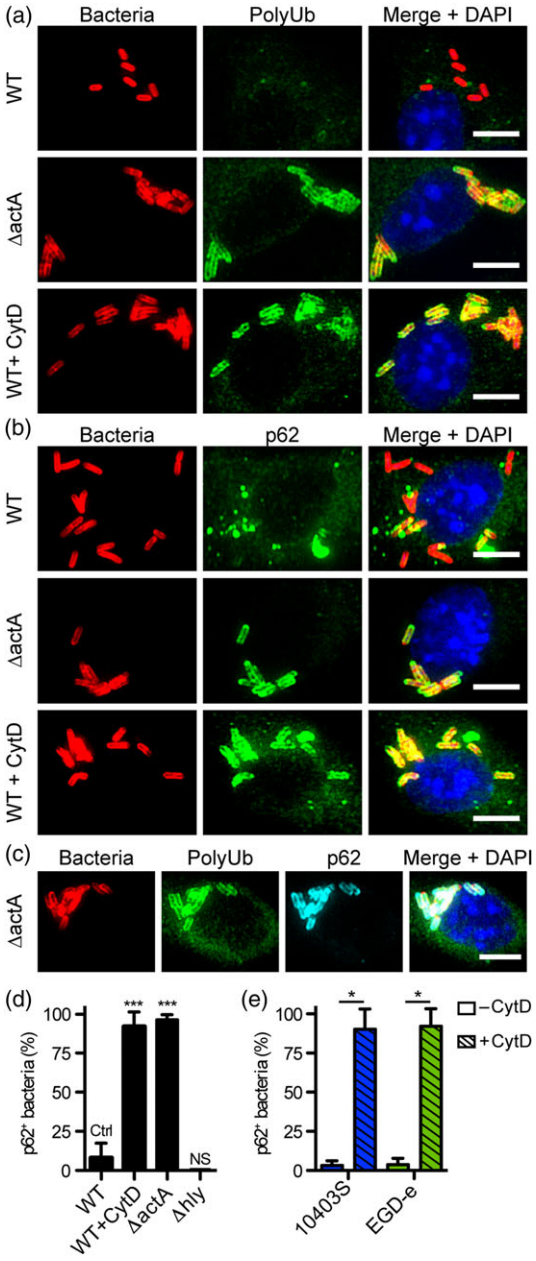

FIGURE 1 Inhibition of actin polymerisation with cytochalasin D (CytD) promotes ubiquitylation of *L. monocytogenes* and the recruitment of p62 during macrophage infection. BMMs were treated with 250 ng/ml CytD 30 min prior to infection, and samples were stained at 3-hr post-infection. Representative micrographs of BMMs infected with WT (10403S), Δ*actA*, and WT in presence of CytD and stained for *L. monocytogenes* (red), polyubiquitylated (polyUb) proteins (a) or p62 (b; green) and DNA (blue). (c) Representative micrographs of BMMs infected with Δ*actA* and stained for *L. monocytogenes* (red), polyubiquityled proteins (green), p62 (cyan), and DNA (blue). (d) Colocalisation of p62 with WT, WT with CytD treatment, Δ*actA*, and Δ*hly* in BMMs infected for 3 hr (NS = non-significant; ***, $p < .001$ [one-way analysis of variance with Dunnett's post-test using WT as control (Ctrl) group]; $N = 3$). (e) Colocalisation of p62 with *L. monocytogenes* strains 10403S and EGD-e during macrophage infection with or without CytD treatment (*, $p < .05$ [two-tailed unpaired *t* test]; $N = 2$). Proportions of p62$^+$ bacteria are expressed as a percentage of total intracellular bacteria. Results are expressed as means and standard deviations. Scale bars are 5 μm. DAPI = 4′6,-diamidino-2-phenylindole

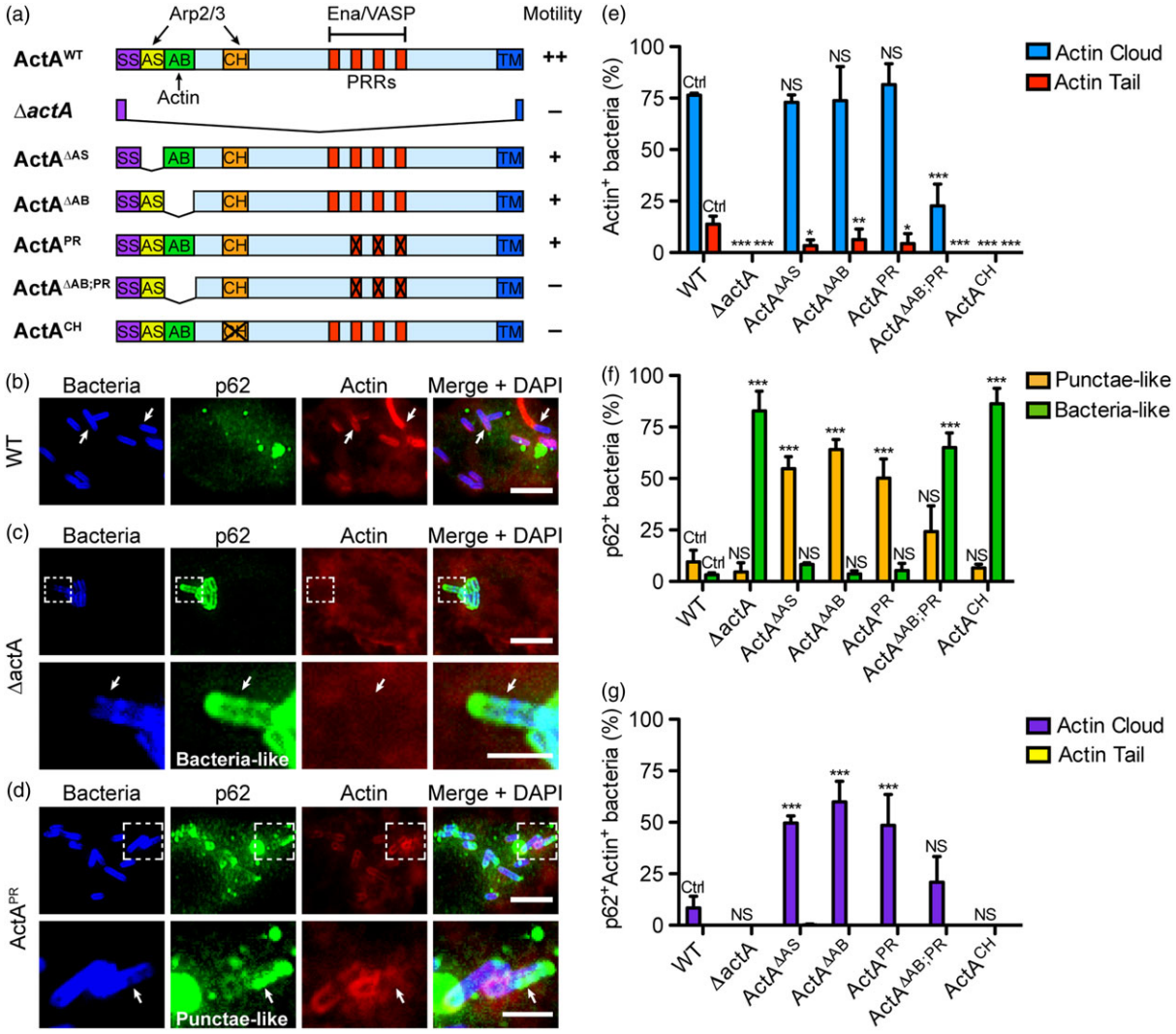

FIGURE 2 ActA mutants colocalise with p62 during macrophage infection. (a) Secondary structures for full-length (ActA^{WT}) and mutant ActA proteins are shown. The functional domains are labelled as "SS" for signal sequence, "AS" acidic stretch, "AB" actin monomer binding site, "CH" cofilin homology domain, "PRRs" proline-rich repeats, and "TM" transmembrane domain. The ActA$^{\Delta AS}$ and ActA$^{\Delta AB}$ mutants have single domain deletions in the AS and the AB, respectively. The ActA^{PR} mutant has proline to glycine substitutions in the three PRRs. The ActA$^{\Delta AB;PR}$ mutant combined the deletion of the actin monomer binding domain with proline to glycine substitutions in the PRR. ActA^{CH} has KKRRK to AAAAA substitutions in the CH. Intracellular motility levels reported for each ActA mutant is indicated on the right. (b–d) BMMs were infected for 3 hr with *L. monocytogenes* strains and stained for bacteria (blue), p62 (green), and actin (red). Selected micrographs are pseudocolored and Z-stacked. (b) BMMs infected with WT bacteria. Arrowheads indicate an actin cloud (left) and an actin tail (right). BMMs infected with Δ*actA* (c) or ActA^{PR} (d) with zoom-in micrographs of selected areas. Arrowheads indicate examples of a bacteria-like p62$^+$ structure (c) and a punctae-like p62$^+$ structure (d). Percentages of bacteria associated with actin clouds and actin tails (e), with punctae-like and bacteria-like p62$^+$ structures (f), or with both p62 and filamentous actin (g) in BMMs infected for 3 hr with WT and ActA mutants (NS = non-significant; *, $p < .05$; **, $p < .01$; ***, $p < .001$ [one-way analysis of variance with Dunnett's post-test using WT as the control (Ctrl)]; $N = 3$). Proportions of positive bacteria are expressed as a percentage of total intracellular bacteria. Results are expressed as means and standard deviations. Scale bars are 2 μm (zoom-in sections in c–d) and 5 μm. DAPI = 4′6,-diamidino-2-phenylindole

at later times of infection. These results showed that, although bacteria with dysfunctional ActA function were completely covered with p62 during macrophage infection, bacteria that polymerised actin only transiently colocalised with punctae-like p62$^+$ structures.

Autophagy receptors (e.g., p62) mediate the engulfment of microbes by autophagic membranes decorated by the autophagy protein LC3. To determine if ActA-mediated actin polymerisation interferes with the targeting of *L. monocytogenes* by autophagic membranes, colocalisation of ActA mutants with LC3 was assessed during macrophage infection. Increased levels of LC3 colocalisation were observed in macrophages infected with strongly impaired ActA mutants (Δ*actA*, ActA$^{\Delta AB;PR}$, and ActA^{CH}) in comparison with macrophages infected with WT bacteria (Figure 4a,b). No differences in colocalisation with LC3 were observed between macrophages infected with WT and the weakly impaired ActA mutants (ActA$^{\Delta AS}$, ActA$^{\Delta AB}$, and ActA^{PR}; Figure 4a,b). These results showed that only strains with strongly impaired ability to mediate actin polymerisation associated with LC3$^+$ membranes. Taken together, these results suggested that *L. monocytogenes* exploits actin polymerisation to evade recognition by the autophagy machinery during macrophage infection.

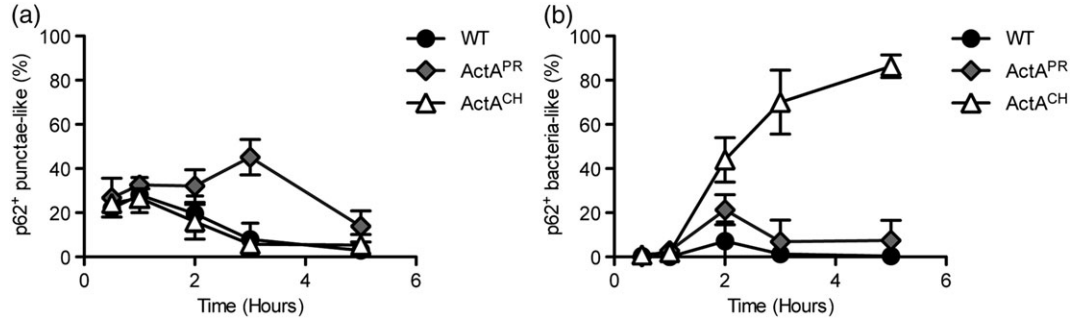

FIGURE 3 Kinetics of colocalisation of *L. monocytogenes* with punctae-like and bacteria-like p62$^+$ structures during macrophage infection. The colocalisation of WT, the weakly impaired mutant ActA^{PR}, and the strongly impaired mutant ActA^{CH} with punctae-like (a) and bacteria-like (b) p62$^+$ structures were evaluated as a function of time during macrophage infection (N = 3). Proportions of p62$^+$ bacteria are expressed as a percentage of total intracellular bacteria. Results are expressed as means and standard deviations

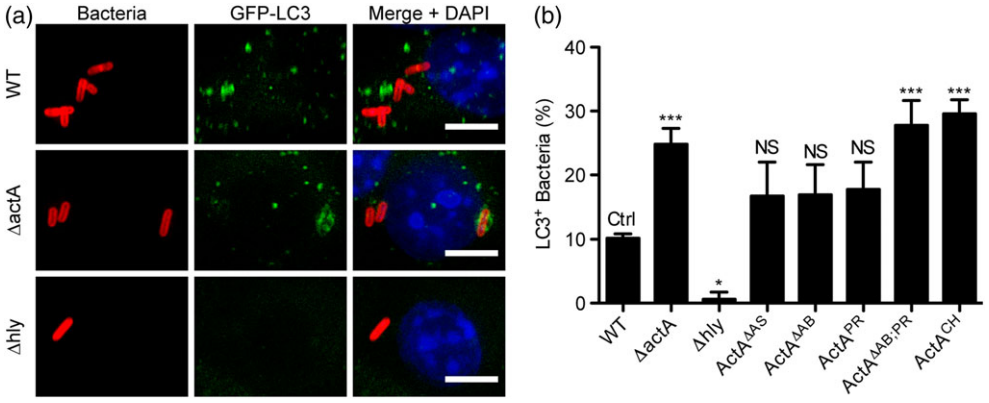

FIGURE 4 ActA mutants colocalise with LC3 during macrophage infection. (a) Representative micrographs of green fluorescent protein (GFP)-LC3 bone marrow-derived macrophages infected with WT, Δ*actA*, and Δ*hly* for 2 hr and stained for *L. monocytogenes* (red), GFP-LC3 (green), and DNA (blue). (b) Colocalisation of GFP-LC3 in bone marrow-derived macrophages infected for 2 hr with WT, Δ*hly*, and ActA mutants (NS = non-significant; *, p < .05; ***, p < .001 [one-way analysis of variance with Dunnett's post-test using WT as the control (Ctrl)]; N = 3). Proportions of GFP-LC3$^+$ bacteria are expressed as a percentage of total intracellular bacteria. Results are expressed as means and standard deviations. Scale bars are 5 μm. DAPI = 4′6,-diamidino-2-phenylindole

2.3 | Activation of actin polymerisation by ActA promotes autophagy avoidance and growth of PLC mutants in macrophages

Although ActA is not required for intracellular growth, a triple mutant lacking ActA, PlcA, and PlcB is subject to autophagy and fails to grow in macrophages (Mitchell et al., 2018). To test the hypothesis that ActA-mediated actin polymerisation interferes with growth-restricting autophagy, PLC-minus strains (hereafter referred to as PlcAB$^-$) carrying mutations in ActA that strongly (ActA$^{\Delta AB;PR}$ and ActA^{CH}) or weakly (ActA$^{\Delta AB}$ and ActA^{PR}) impaired actin polymerisation and actin-based motility were constructed (See Experimental Procedures). The intracellular growth of these ActA mutants was evaluated in macrophages (Figure 5a,b). In a PLC-deficient background, weakly impaired ActA mutants (ActA$^{\Delta AB}$ and ActA^{PR}) grew similarly to a strain with a WT *actA* allele (Figure 5a). In contrast, the growth of PlcAB$^-$ strains carrying mutations that strongly impaired actin polymerisation (Δ*actA*, ActA$^{\Delta AB;PR}$, and ActA^{CH}) grew similarly to PlcAB$^-$ strain carrying a Δ*actA* allele (Figure 5 b). These results demonstrated that ActA-mediated actin polymerisation promoted growth of PLC-deficient strains during macrophage infection.

To confirm that the growth defect of PlcAB$^-$ strains carrying mutations that strongly impaired actin polymerisation (Δ*actA*, ActA$^{\Delta AB;PR}$, and ActA^{CH}) was due to autophagy, the intracellular growth of these strains was monitored in macrophages that lack ATG5, a core subunit necessary for autophagosome formation. As expected, the intracellular growth defect of these PlcAB$^-$ strains carrying strongly impaired *actA* alleles was rescued to the level of WT in *Atg5*$^{-/-}$ cells (Figure 5c), indicating that functional autophagy is required to restrict their growth in macrophages. The extent of the targeting of these mutants by autophagy was further characterised by quantifying their colocalisation with LC3 during macrophage infection (Figure 5d). PlcAB$^-$ strains carrying mutations that strongly impaired actin polymerisation (Δ*actA*, ActA$^{\Delta AB;PR}$, and ActA^{CH}) showed a marked increase in LC3 colocalisation in comparison with mutants with a WT *actA* allele or the weakly impaired ActA mutants (ActA$^{\Delta AB}$ and ActA^{PR}; Figure 5d). Overall, these results showed that the activation of actin polymerisation by ActA interfered with growth-restricting autophagy.

2.4 | Actin-based motility allows *L. monocytogenes* to escape from LC3$^+$ membranes

Results from previous sections indicated that actin-based motility may play a role in the avoidance of *L. monocytogenes* from autophagy (Figures 2g and 3). To test this hypothesis, the kinetics of *L. monocytogenes* that colocalised with green fluorescent protein (GFP)-LC3 during macrophage infection was monitored using time-lapse

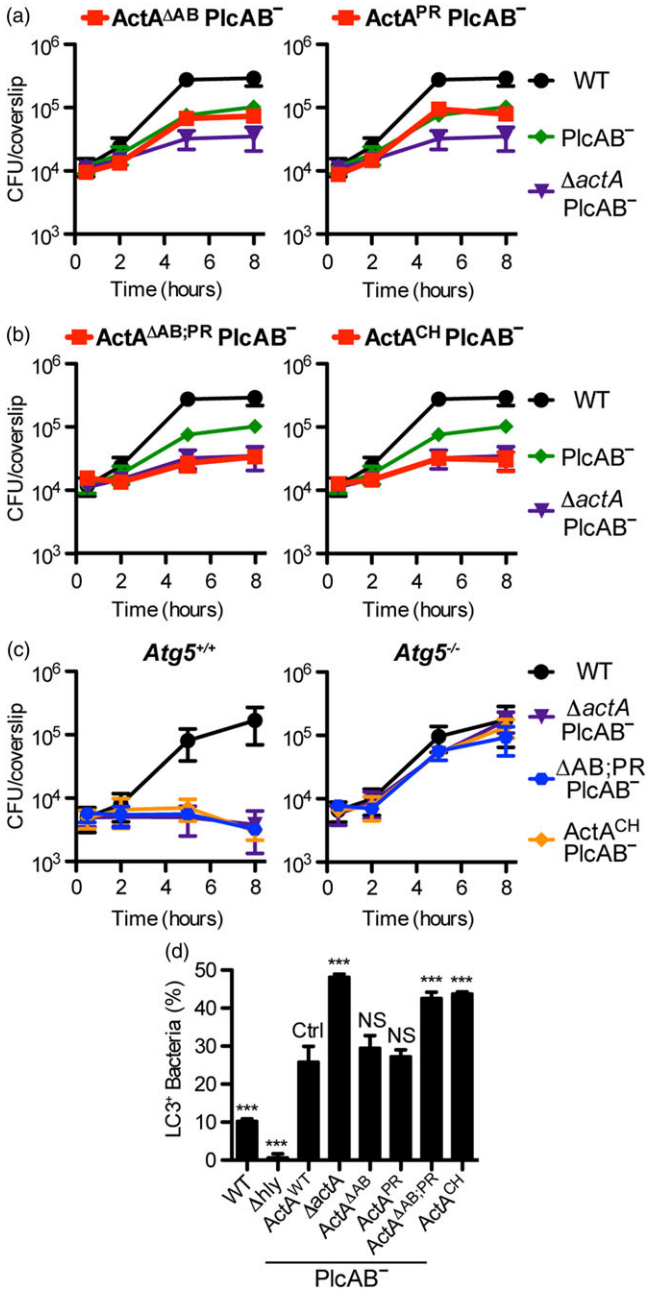

FIGURE 5 Activation of actin polymerisation by ActA promotes autophagy avoidance and growth of phospholipase C (PLC) mutants in macrophages. Intracellular bacterial growth kinetics for BMMs infected with WT, PlcA^{H86A} PlcB^{H69G} (PlcAB$^-$), Δ*actA* PlcAB$^-$, and weakly impaired (ActA$^{\Delta AB}$ PlcAB$^-$ and ActA^{PR} PlcAB$^-$; a) or strongly impaired (ActA$^{\Delta AB;PR}$ PlcAB$^-$ and ActA^{CH} PlcAB$^-$; b) ActA mutant strains (N = 3). The same data are represented for the control strains WT, PlcAB$^-$, and Δ*actA* PlcAB$^-$ in (a) and (b). (c) Intracellular bacterial growth kinetics for *Atg5*$^{+/+}$ and *Atg5*$^{-/-}$ BMMs infected with WT, Δ*actA* PlcAB$^-$, ActA$^{\Delta AB;PR}$ PlcAB$^-$, and ActA^{CH} PlcAB$^-$ (N = 4). (d) Colocalisation of GFP-LC3 in BMMs infected for 2 hr with WT, Δ*hly*, and indicated ActA mutants in a PlcAB$^-$ background (NS = non-significant; ***, p < .001 [one-way analysis of variance with Dunnett's post-test using WT as the control (Ctrl)]; N = 3). The same data are represented for the control strains WT and Δ*hly* in Figure 4b and 5d. Proportions of GFP-LC3$^+$ bacteria are expressed as a percentage of total intracellular bacteria. Results are expressed as means and standard deviations. CFU = colony-forming unit

microscopy. GFP-LC3 was transiently recruited to the entry vacuole of WT bacteria early during infection. WT bacteria subsequently escaped from GFP-LC3$^+$ membranes and began moving and efficiently proliferated in the host cytosol (Figure 6a and Movies S1 and S2). Similarly, GFP-LC3$^+$ membranes from the entry vacuole dissociated from Δ*actA*, which then replicated without moving and formed microcolonies. Although Δ*actA* was usually not engulfed by GFP-LC3$^+$ membranes in the host cytosol, GFP-LC3$^+$ punctae often localised in close proximity to microcolonies (Figure 6b and Movies S3 and S4), which confirms that PLCs are sufficient to inhibit antibacterial autophagy in the macrophage cytosol. The PlcAB$^-$ mutant associated with GFP-LC3 for a longer period of time than WT and Δ*actA* and was often targeted sequentially by distinct autophagic events (Figure 6c and Movies S5 and S6), as previously reported for Δ*actA* PlcAB$^-$ (Figure 6d and Movies S7 and S8; Mitchell et al., 2018). However, in contrast to the Δ*actA* PlcAB$^-$ strain, some PlcAB$^-$ bacteria escaped subsequent retargeting by autophagy and moved away from the subcellular region in which bacteria colocalised with LC3$^+$ membranes (Figure 6c and Movies S5 and S6). Similar to Δ*actA* PlcAB$^-$, the PlcAB$^-$ strain carrying a mutation in the cofilin homology sequence (ActA^{CH} PlcAB$^-$), which strongly impaired ActA-mediated actin polymerisation and actin-based motility, frequently associated with GFP-LC3 during infection (Figure 6e and Movies S9 and S10). Taken together, these results suggested that actin-based motility allowed *L. monocytogenes* to move away from subcellular areas in which bacteria colocalised with autophagic membranes. In addition, these results confirmed that PLCs acted on LC3$^+$ membranes from the entry vacuole but also interfered with subsequent retargeting of cytosolic bacteria by autophagy.

The role of actin polymerisation and actin-based motility in the avoidance of *L. monocytogenes* from autophagy was further studied using time-lapse microscopy and a probe that stained F-actin during infection of GFP-LC3 macrophages. As previously observed (Figure 6a and Movies S1 and S2), WT bacteria escaped from LC3$^+$ entry vacuoles, replicated in the cytosol, and performed actin-based motility (Figure 7a and Movie S11). The ability of WT *L. monocytogenes* to activate actin polymerisation was observed using the fluorescent actin probe through the formation of actin clouds and actin tails (Figure 7a and Movie S11). Surprisingly, during infection of macrophages with the PlcAB$^-$ strain, F-actin was recruited within LC3$^+$ entry vacuoles preceding its collapse and the escape of bacteria in the host cytosol (Figure 7b and Movies S12 and S13). This suggested that *L. monocytogenes* might use actin polymerisation to burst out of vacuoles more efficiently. Importantly, nonmotile PlcAB$^-$ bacteria were subsequently retargeted by distinct autophagy events, and bacteria that performed actin-based motility were protected from targeting by LC3$^+$ membranes. These results further supported the hypothesis that actin-based motility allows *L. monocytogenes* to escape autophagosomal membranes during macrophage infection.

3 | DISCUSSION

The results of this study demonstrated that *L. monocytogenes* exploits actin polymerisation and actin-based motility to avoid autophagy during infection of macrophages. The data showed that intracellular

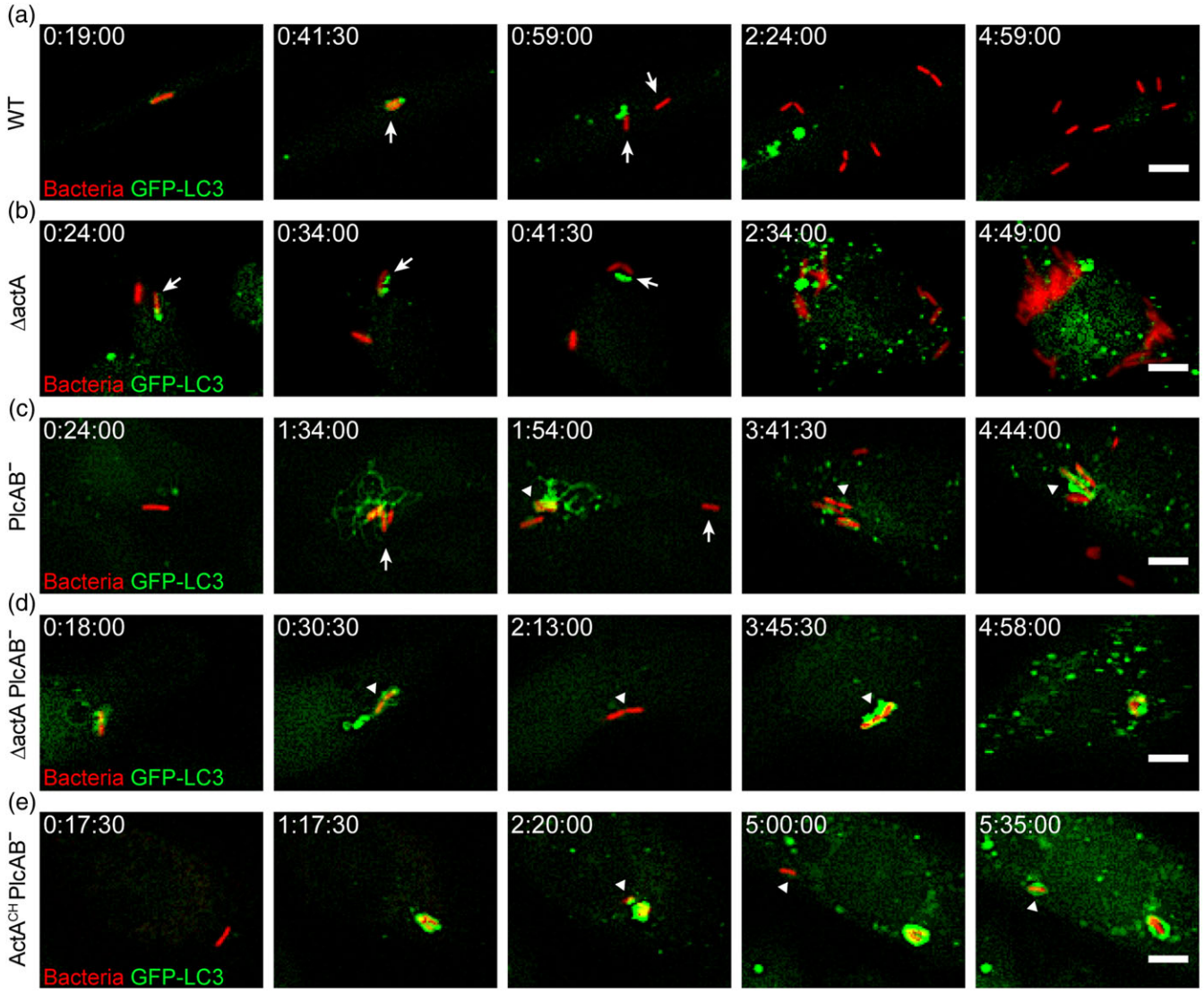

FIGURE 6 ActA allows *L. monocytogenes* to escape from LC3$^+$ membranes and to avoid subsequent retargeting by autophagy. Time-lapse microscopy of green fluorescent protein (GFP)-LC3 (green) BMMs infected with various strains of *L. monocytogenes* expressing mCherry (red). Selected Z-stacked micrographs are shown for various time points. (a) GFP-LC3 BMMs infected with WT bacteria. Arrowheads indicate bacteria that removed GFP-LC3$^+$ membrane, moved away, and replicated in the host cytosol. (b) GFP-LC3 BMMs infected with Δ*actA* bacteria. Arrowheads indicate bacteria that removed GFP-LC3$^+$ membrane and replicated in the cytosol. (c) GFP-LC3 BMMs infected with PlcAB$^-$ bacteria. Arrowheads indicate a bacterium that moved away from GFP-LC3$^+$ membranes and was no longer targeted by autophagy. GFP-LC3 BMMs infected with Δ*actA* PlcAB$^-$ (d) or ActA^{CH}PlcAB$^-$ (e) bacteria. Triangles indicate bacteria that were retargeted by autophagy (c–e). Times are indicated (hr:min:s) at the top-left corner of each micrograph. Scale bars are 5 μm

L. monocytogenes that polymerised actin was protected from ubiquitylation and from the recruitment of the autophagy receptor p62 and autophagic membranes. This study also revealed a role for actin polymerisation in avoiding growth-restricting autophagy in strains lacking PLCs, which are the dominant factors mediating autophagy avoidance in *L. monocytogenes*. Results from time-lapse microscopy experiments suggested that actin-based motility allows cytosolic bacteria to move away from subcellular areas with high autophagic activity thereby avoiding subsequent growth restriction. Because several species of pathogens have the ability to use actin polymerisation and perform actin-based motility (Lamason & Welch, 2017; Mitchell et al., 2016), these findings may also be true for other cytosolic bacterial pathogens including *Shigella flexneri*, *Rickettsia* spp., *Burkholderia* spp., and *Mycobacterium marinum* and have a broad impact in the study of infectious diseases and bacterial pathogenesis.

The results of this and other studies show that ActA protects *L. monocytogenes* from recognition by host ubiquitin ligases and autophagy (Mostowy et al., 2011; Perrin et al., 2004; Yoshikawa et al., 2009). However, it is still unclear how the function of ActA in autophagy avoidance is linked to its ability to activate actin polymerisation and how this function is modulated in different cell types. The results from this study expand upon the study from Perrin et al. (2004) to support the hypothesis that *L. monocytogenes* that polymerised actin are protected from ubiquitylation in macrophages. In contrast, Yoshikawa et al. (2009) excluded a role for actin-based motility in autophagy avoidance and showed that ActA interferes with the ubiquitylation of *L. monocytogenes* by coating and masking the

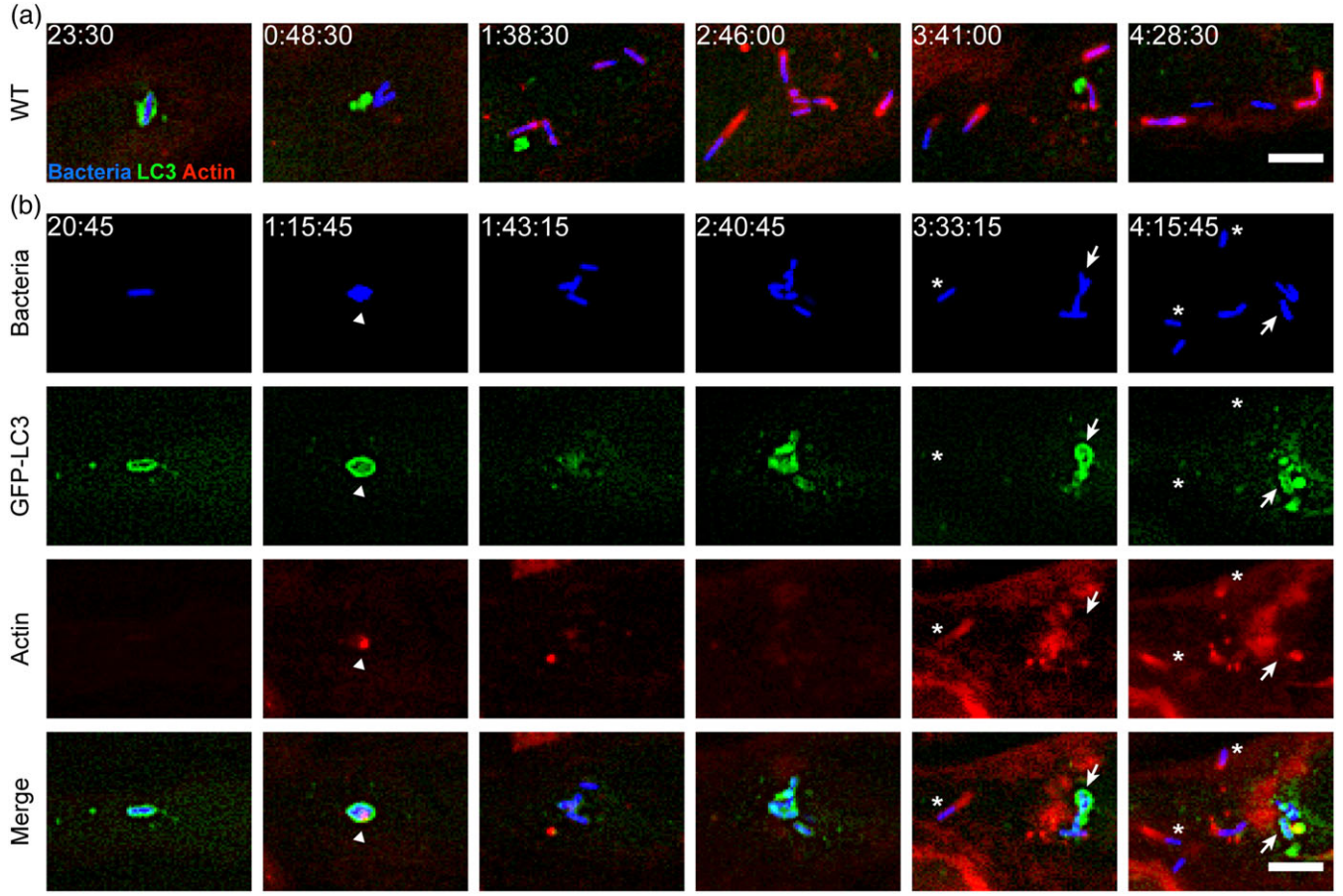

FIGURE 7 Actin-based motility allows *L. monocytogenes* to escape from LC3$^+$ membranes. Time-lapse microscopy of green fluorescent protein (GFP)-LC3 (green) BMMs infected with *L. monocytogenes* expressing mCherry (blue) in presence of a probe for filamentous actin (red). Selected pseudo-coloured Z-stacked micrographs are shown for various time-points. (a) GFP-LC3 BMMs infected with WT bacteria. (b) GFP-LC3 BMMs infected with PlcAB$^-$ bacteria. Triangles indicate actin that strongly localised within a GFP-LC3$^+$ *L. monocytogenes*-containing vacuole. Asterisks indicate bacteria that polymerised actin and moved away from GFP-LC3$^+$ membranes. Arrowheads indicate nonmotile bacteria that colocalised with GFP-LC3. Between time-points 1:43:15 and 2:40:45, nonmotile bacteria were retargeted by GFP-LC3. Times are indicated (hr:min:s) at the top-left corner of each selected micrograph. Scale bars are 5 μm

bacterial surface with host proteins during infection of epithelial cells. An explanation for these apparent discrepancies is that actin polymerisation is important to protect cytosolic bacteria against autophagy in certain subsets of host cells (e.g., macrophages) but not in others (e.g., epithelial cells and fibroblasts; Figure S1). In accordance with this hypothesis, the ability to polymerise actin seemed to interfere with the ubiquitylation of *M. marinum* in macrophages (Collins et al., 2009) but did not protect *S. flexneri* from autophagy during infection of epithelial cells (Ogawa et al., 2005). On the other hand, the cytosolic bacterial pathogen *Francisella tularensis* does not exhibit actin-based motility and requires the bacterial surface O-antigen polysaccharides to avoid ubiquitylation during macrophage infection (Case et al., 2014). Therefore, the strategies used by cytosolic bacterial pathogens to avoid autophagic recognition vary across species and might be optimised for the infection of specific host cells. Given the wide range of cells infected by *L. monocytogenes*, one possibility is that ActA promotes autophagy avoidance by both blocking host access to the bacterial surface and by activating the actin polymerisation machinery. These different mechanisms of autophagy avoidance could confer varying levels of protection depending on the cell type being infected by *L. monocytogenes*.

How might actin polymerisation interfere with the recognition of *L. monocytogenes* by autophagy during infection? It is possible that actin polymerisation in the vicinity of cytosolic bacteria protects the bacterial surface from autophagic recognition by blocking access to ubiquitin ligases and autophagy receptors. However, it is clear that cytosolic bacteria that form actin comet tails do not undergo ubiquitylation in macrophages (this study, Collins et al., 2009, and Perrin et al., 2004), which suggests that actin-based motility protects cytosolic bacteria from autophagic recognition. In addition, our results showed that in the absence of PLCs, *L. monocytogenes* used actin polymerisation not only to escape from the entry vacuole, as previously suggested by Poussin and Goldfine (2010), but also to move away from LC3$^+$ membranes using actin-based motility (Figures 6 and 7). However, it is not clear whether the interference of ActA with autophagic recognition and with the subsequent entrapment of bacteria by autophagic membranes are codependent phenomena. Although it is conceivable that actin-based motility allows intracellular bacteria to avoid entrapment by autophagic membranes, it is more difficult to explain how actin-based motility might protect from the action of ubiquitin ligases and the recruitment of autophagy receptors. We speculate that a certain period of time is required for the host cell to

mount a localised response against a cytosolic bacterium. In this scenario, moving *L. monocytogenes* would not spend enough time at any given subcellular region to be efficiently detected and tagged for autophagic degradation. It is also possible that ubiquitin ligases that act on cytosolic bacteria are compartmentalised and that *L. monocytogenes* exploits actin-based motility to escape from those specific subcellular regions of the host cell.

Beyond their function in antimicrobial autophagy, ubiquitin chains, autophagy receptors (e.g., p62), and ATG8 family proteins (e.g., LC3) might have a broader function and act as molecular tags that mark microbial invaders, allowing the recruitment of host components involved in various antimicrobial processes. For example, markers involved in autophagy also recruit interferon-regulated GTPases known to promote lysis of pathogen-containing vacuoles and cytosolic microbes (Mitchell & Isberg, 2017). In addition, ubiquitylated proteins mediate the recruitment of the proteasome to cytosolic *Salmonella enterica* serovar Typhimurium (*S.* Typhimurium; Perrin et al., 2004) and *Mycobacterium tuberculosis*-associated structures (Franco et al., 2017). However, the molecular mechanisms and exact consequences of this recruitment remain to be determined. The decoration of the bacterial surface with ubiquitin chains may also act as a signalling platform that promotes the secretion of proinflammatory cytokines and autophagy-independent restriction of cytosolic bacteria, as shown for *S.* Typhimurium (Noad et al., 2017; van Wijk et al., 2017). The interference of microbial pathogens with the recruitment of proteins involved in antimicrobial autophagy might then be part of a broader strategy to counteract host cell-autonomous defences and fine-tune the immune response.

Distinguishing antimicrobial autophagy from other host autophagic processes might lead to the development of host-targeted therapies to combat infectious diseases. The identification of ubiquitin ligases that selectively mark microbial pathogens will constitute one step towards delineating the unique features of antimicrobial autophagy and host cell-autonomous defence mechanisms. Ubiquitin ligases that target cytosolic *S.* Typhimurium (Huett et al., 2012; Noad et al., 2017; van Wijk et al., 2017) and *M. tuberculosis*-containing vacuoles (Franco et al., 2017; Manzanillo et al., 2013) have already been identified, but their spectrum of action remains to be further studied, and their host or bacterial substrates are unknown. Importantly, microbial substrates for ubiquitylation might represent excellent targets for the development of antimicrobials and vaccines, because the immune system usually recognises conserved microbial molecular patterns.

4 | EXPERIMENTAL PROCEDURES

4.1 | Bacterial strains, cell growth medium, and cell culture

The *L. monocytogenes* strains used in this study are listed in Table 1. All mutant strains were derived from 10403S (Becavin et al., 2014), including Δ*hly* (Jones & Portnoy, 1994). Strains were grown in brain heart infusion broth at 30 °C overnight prior to each experiment unless otherwise specified. BMMs were prepared and cultured using standard procedures, as previously described (Mitchell et al., 2015). $Atg5^{flox/flox}$, $Atg5^{flox/flox}$-LysM-*cre*, and GFP-LC3 mice were previously described (Martinez et al., 2015; Watson, Manzanillo, & Cox, 2012). MEFs were obtained from The University of California, Berkeley Cell Culture facility and were grown at 37 °C and 5% CO_2 in Dulbecco's modified Eagle's medium supplemented with 10% fetal bovine serum, 2 mM L-glutamine, and 1 mM sodium pyruvate.

4.2 | Intracellular growth curves

Intracellular growth curves were performed, as previously described (Mitchell et al., 2015). BMMs were infected at a multiplicity of infection (MOI) of 0.25 (one bacterium per four macrophages), resulting in approximately 8% infected cells. At 30 min post-infection, cells were washed, and fresh medium was added. At 1 hr post-infection, 50 μg/ml of gentamicin was added to kill extracellular bacteria. Intracellular bacteria were quantified by enumerating colony-forming units at various time points.

4.3 | Immunofluorescence, microscopy, and image analysis

BMMs were infected at a MOI of 0.4 (two bacteria per five macrophages), resulting in 13% infected cells, as previously described for the intracellular growth curves. MEF cells were infected with an MOI of 150, washed with phosphate buffered saline (PBS) at 1 hr post-infection, and incubated in media containing 50 μg/ml of gentamicin. When specified, 250 ng/ml of cytochalasin D (Sigma, St. Louis, MO, USA) was added 30 min prior to infection. At the time points indicated in figure legends, coverslips were washed twice with PBS and fixed with 4% paraformaldehyde for 15 min. Then, coverslips were incubated for 30 min in permeabilisation/blocking buffer (PB buffer; PBS containing 2% bovine serum albumin and 0.1% Saponin). Primary antibodies that recognise *L. monocytogenes* (BD Biosciences, San Jose, CA, USA; no. 223021; 1:1,000 dilution), p62 (Fitzgerald, Acton, MA, USA; no. 20R-PP001; 1:200 dilution), polyubiquitin chains (Enzo Life Sciences, Farmingdale, NY, USA; FK1, no. PW8805; 1:200 dilution), or GFP (Roche, Basel, Switzerland; no. 11814460001; 1:200 dilution) were diluted in PB buffer, added to coverslips, and incubated for 90 min. The coverslips were washed 6 times with 0.1% Saponin in PBS. The secondary antibodies AlexaFluor-488 goat anti-mouse IgG (Invitrogen, Carlsbad, CA, USA; no. A11029; 1:2,000 dilution), AlexaFluor-488 goat anti-mouse IgM (Invitrogen; no. A21042, 1:2,000 dilution), rhodamine red-X goat anti-rabbit IgG (Invitrogen; no. R6394, 1:2,000 dilution) and AlexaFluor-647 goat anti-guinea pig IgG (Invitrogen; no. A21450; 1:2,000 dilution), and phalloidin AlexaFluor-488 (Invitrogen; no. A12379; 1:500 dilution) or phalloidin AlexaFluor-647 (Invitrogen; no. A22287; 1:500 dilution) were diluted in PB buffer, added to coverslips, and incubated for 1 hr. Coverslips were washed 3 times in 0.1% Saponin in PBS and 3 times in PBS and dried for 1 hr before mounting in a drop of ProLong Gold antifade reagent containing 4′ 6,-diamidino-2-phenylindole (Invitrogen). Imaging was performed on an Olympus IX71 epifluorescence microscope or a KEYENCE BZ-X710 fluorescent microscope using a 100× objective. For each condition, several frames were selected randomly and colour

TABLE 1 *Listeria monocytogenes* strains used in this study

Strain	Description	Reference or source
10403S	Wild type	Becavin et al. (2014)
DP-L6573	10403S pHPL3-mCherry	Vincent et al. (2016)
DP-L3633	EGD-e	Becavin et al. (2014)
DP-L2161	Δ*hly*	Jones and Portnoy (1994)
DP-L3078	Δ*actA* (ActA$^{\Delta 7-633}$)	Skoble et al. (2000)
DP-L6597	DP-L3078 pHPL3-mCherry	This study
DP-L3996	ActA$^{\Delta 31-58}$ (ActA$^{\Delta AS}$)	Skoble et al. (2000)
DP-L3994	ActA$^{\Delta 60-101}$ (ActA$^{\Delta AB}$)	Skoble et al. (2000)
DP-L4032	ActA$^{PPP > GGG}$ (ActA^{PR})	Skoble et al. (2001)
DP-L4236	ActA$^{\Delta 60-101;PPP > GGG}$(ActA$^{\Delta AB;PR}$)	Skoble et al. (2001)
DP-L4110	ActA$^{KKRRK > AAAAA}$ (ActA^{CH})	Lauer et al. (2001)
DP-L3430	PlcA^{H86A}	Bannam and Goldfine (1999)
DP-L3177	PlcB^{H69G}	Zuckert et al. (1998)
DP-L6598	ActA$^{\Delta AB}$ PlcB^{H69G}	This study
DP-L6599	ActA^{PR} PlcB^{H69G}	This study
DP-L6600	ActA$^{\Delta AB;PR}$ PlcB^{H69G}	This study
DP-L6601	ActA^{CH} PlcB^{H69G}	This study
DP-L6579	PlcA^{H86A} PlcB^{H69G} (PlcAB^{-})	Mitchell et al. (2018)
DP-L6602	DP-L6579 pHPL3-mCherry	This study
DP-L6586	Δ*actA* PlcAB^{-}	Mitchell et al. (2018)
DP-L6587	DP-L6586 pHPL3-mCherry	Mitchell et al. (2018)
DP-L6603	ActA$^{\Delta AB}$ PlcAB^{-}	This study
DP-L6604	ActA^{PR} PlcAB^{-}	This study
DP-L6605	ActA$^{\Delta AB;PR}$ PlcAB^{-}	This study
DP-L6606	ActA^{CH} PlcAB^{-}	This study
DP-L6607	DP-L6606 pHPL3-mCherry	This study

combined using the MetaMorph software (Universal imaging) or the BZ-X analyser software. Images showed in Figures 1, 2, and 4 were obtained by stacking at least 10 layers covering 5 μm of thickness and post-treated using the haze reduction function of the BZ-X analyser software. Images from at least three independent experiments (unless otherwise specified) were analysed using ImageJ (National Institutes of Health, USA). A minimum of 100 bacteria were quantified for each condition.

4.4 | Plasmids and strain construction

Plasmid DNA isolation and purification of DNA fragments were performed according to manufacturers' recommendations (QIAGEN, Redwood City, CA). Polymerase chain reactions (PCRs) were performed using Kapa polymerase (Kapa Biosystems, Wilmington, MA, USA). Unless otherwise stated, all other molecular reagents were purchased from New England Biolabs (Ipswich, MA, USA).

Escherichia coli SM10 (Simon, Priefer, & Puhler, 1983) carrying pKSV7-*oriT* PlcB^{H69G} (DP-E6570; Mitchell et al., 2018; Zuckert, Marquis, & Goldfine, 1998) was conjugated into ActA$^{\Delta AB}$ (DP-L3994), ActA^{PR} (DP-L4032), ActA$^{\Delta AB;PR}$ (DP-L4236), and ActA^{CH} (DP-L4110) and used to generate ActA$^{\Delta AB}$ PlcB^{H69G} (DP-L6598), ActA^{PR} PlcB^{H69G} (DP-L6599), ActA$^{\Delta AB;PR}$ PlcB^{H69G} (DP-L6600), and ActA^{CH} PlcB^{H69G} (DP-L6601) through allelic replacement, as previously described (Whiteley et al., 2017). The plasmid pKSV7-*oriT* PlcA^{H86A} was generated by amplifying *plcA* from PlcA^{H86A} (DP-L3430; Bannam & Goldfine, 1999) using colony PCR and the primers GM1113 (5′-ATATATGTCGACTGGGTTTCACTCTCCTTCTAC-3′) and GM0064 (5′-ATATATGGTACCAGAGTTAGTATATGGTTCCGAGG-3′). The PCR product was then digested with SalI and KpnI and ligated into pKSV7-*oriT* (Whiteley et al., 2017) using the T4 DNA ligase. The ligation product was transformed in chemically competent Mach1 *E. coli* (Thermo Fischer Scientific, Waltham, MA, USA), and positive clones were confirmed by PCR and Sanger sequencing. Plasmid were transferred into *E. coli* SM10 (thus generating DP-E6608) and then conjugated into DP-L6598, DP-L6599, DP-L6600, and DP-L6601 in order to generate ActA$^{\Delta AB}$ PlcA^{H86A} PlcB^{H69G} (DP-L6603), ActA^{PR} PlcA^{H86A} PlcB^{H69G} (DP-L6604), ActA$^{\Delta AB;PR}$ PlcA^{H86A} PlcB^{H69G} (DP-L6605), and ActA^{CH} PlcA^{H86A} PlcB^{H69G} (DP-L6606) using an allelic replacement protocol (Whiteley et al., 2017).

E. coli SM10 carrying pHPL3-mCherry (Vincent, Freisinger, Lam, Huttenlocher, & Sauer, 2016) was conjugated with Δ*actA* (DP-L3078), PlcA^{H86A}PlcB^{H69G} (DP-L6579), and ActA^{CH} PlcA^{H86A} PlcB^{H69G} (DP-L6606), as previously described (Lauer, Chow, Loessner, Portnoy, & Calendar, 2002).

4.5 | Time-lapse microscopy

GFP-LC3 BMMs were seeded in 35-mm dishes (MatTek, Ashland, MA; P35GC-1.5-14-C) using 1 × 10^6 cells in media without phenol red.

Overnight cultures of *L. monocytogenes* strains expressing mCherry were diluted 1:12 in brain heart infusion broth and incubated for 1 hr 45 min at 37 °C with shaking. The bacterial cultures were then washed and diluted 1:500 before infecting macrophages for 3 min. Infected cells were washed 3 times with PBS, and imaging was performed in media without phenol red containing a 1:100 dilution of ProLong Antifade Reagents for Live Cells (Invitrogen).

A silicone rhodamine (SiR)-actin probe (Cytoskeleton, Denver, CO, USA; CY-SC001) was used to visualise actin dynamic in live cells, following manufacturer's recommendations. Briefly, GFP-LC3 BMMs were pretreated 1 hr prior to infection with 1 μM SiR-actin probe and 10 μM verapamil (Cytoskeleton), an efflux pump inhibitor used to enhance probe retention and staining. Live imaging was performed in the presence of 100 nM SiR-actin probe and 10 μM verapamil for the duration of the experiment.

Time-lapse microscopy experiments were performed using a KEYENCE BZ-X710 fluorescence microscope equipped with an incubation chamber at 37 °C with 5% CO_2 using the focus tracking functionality. For each XY position and time point, images from five Z-layers covering 5 μm of thickness were acquired with a 100× objective. Images were Z-stacked and post-treated using the haze reduction function of the BZ-X analyser software. The colour balance of micrographs presented in Figures 6 and 7 were uniformly adjusted across specific experiments using ImageJ.

4.6 | Ethical statement

This study was performed in accordance with the Guide for the Care and Use of Laboratory Animals of the National Institutes of Health (National Research Council, 1996). Protocols were approved by the Animal Care and Use Committee of the University of California, Berkeley.

4.7 | Statistical analysis

GraphPad Prism software (v.7.00) was used to perform statistical analysis. Specific statistical tests and number of independent experiments carried out are indicated in each figure legend.

ACKNOWLEDGEMENTS

We thank Jeff Cox (UC Berkeley) for generously providing us with mouse femurs and Matt Welch (UC Berkeley) for helpful advice. This work was supported by National Institutes of Health grants 1P01 AI063302 (D. A. P.) and 1R01 AI027655 (D. A. P.) and by the Defense Threat Reduction Agency grant HDTRA1-13-1-0003 (C. C. and D. A. P.). G. M. was supported by fellowships from Fonds de recherche du Québec - Nature et technologies (FRQNT), Fonds de recherche du Québec - Santé (FRQS), and the Natural Sciences and Engineering Research Council of Canada (NSERC). Fellowships from the Olle Engkvist Byggmästare foundation (Stiftelsen Olle Engkvist Byggmästare; Sweden), the Swedish Society of Medical Research (Svenska Sällskapet för Medicinsk Forskning), and the Sweden-America Foundation supported P. E.

Daniel A. Portnoy has a consulting relationship with and a financial interest in Aduro Biotech. Both he and the company stand to benefit from the commercialisation of the results of this research.

ORCID

Mandy I. Cheng http://orcid.org/0000-0002-8915-0296
Chen Chen http://orcid.org/0000-0003-3862-062X
Patrik Engström http://orcid.org/0000-0003-3092-8216
Gabriel Mitchell http://orcid.org/0000-0001-7977-5316

REFERENCES

Auerbuch, V., Loureiro, J. J., Gertler, F. B., Theriot, J. A., & Portnoy, D. A. (2003). Ena/VASP proteins contribute to Listeria monocytogenes pathogenesis by controlling temporal and spatial persistence of bacterial actin-based motility. *Molecular Microbiology*, *49*, 1361–1375.

Bannam, T., & Goldfine, H. (1999). Mutagenesis of active-site histidines of Listeria monocytogenes phosphatidylinositol-specific phospholipase C: Effects on enzyme activity and biological function. *Infection and Immunity*, *67*, 182–186.

Becavin, C., Bouchier, C., Lechat, P., Archambaud, C., Creno, S., Gouin, E., … Cossart, P. (2014). Comparison of widely used Listeria monocytogenes strains EGD, 10403S, and EGD-e highlights genomic variations underlying differences in pathogenicity. *MBio*, *5*, e00969–e00914.

Case, E. D., Chong, A., Wehrly, T. D., Hansen, B., Child, R., Hwang, S., … Celli, J. (2014). The Francisella O-antigen mediates survival in the macrophage cytosol via autophagy avoidance. *Cellular Microbiology*, *16*, 862–877.

Choy, A., & Roy, C. R. (2013). Autophagy and bacterial infection: An evolving arms race. *Trends in Microbiology*, *21*, 451–456.

Collins, C. A., De Maziere, A., van Dijk, S., Carlsson, F., Klumperman, J., & Brown, E. J. (2009). Atg5-independent sequestration of ubiquitinated mycobacteria. *PLoS Pathogens*, *5*, e1000430.

Cossart, P. (2011). Illuminating the landscape of host-pathogen interactions with the bacterium Listeria monocytogenes. *Proceedings of the National Academy of Sciences of the United States of America*, *108*, 19484–19491.

Franco, L. H., Nair, V. R., Scharn, C. R., Xavier, R. J., Torrealba, J. R., Shiloh, M. U., & Levine, B. (2017). The ubiquitin ligase Smurf1 functions in selective autophagy of Mycobacterium tuberculosis and anti-tuberculous host defense. *Cell Host & Microbe*, *22*, 421–423.

Galluzzi, L., Baehrecke, E. H., Ballabio, A., Boya, P., Bravo-San Pedro, J. M., Cecconi, F., … Kroemer, G. (2017). Molecular definitions of autophagy and related processes. *The EMBO Journal*, *36*, 1811–1836.

Gong, L., Devenish, R. J., & Prescott, M. (2012). Autophagy as a macrophage response to bacterial infection. *IUBMB Life*, *64*, 740–747.

Huang, J., & Brumell, J. H. (2014). Bacteria-autophagy interplay: A battle for survival. *Nature Reviews Microbiology*, *12*, 101–114.

Huett, A., Heath, R. J., Begun, J., Sassi, S. O., Baxt, L. A., Vyas, J. M., … Xavier, R. J. (2012). The LRR and RING domain protein LRSAM1 is an E3 ligase crucial for ubiquitin-dependent autophagy of intracellular Salmonella Typhimurium. *Cell Host & Microbe*, *12*, 778–790.

Jones, S., & Portnoy, D. A. (1994). Characterization of Listeria monocytogenes pathogenesis in a strain expressing perfringolysin O in place of listeriolysin O. *Infection and Immunity*, *62*, 5608–5613.

Kimmey, J. M., & Stallings, C. L. (2016). Bacterial pathogens versus autophagy: Implications for therapeutic interventions. *Trends in Molecular Medicine*, *22*, 1060–1076.

Kocks, C., Gouin, E., Tabouret, M., Berche, P., Ohayon, H., & Cossart, P. (1992). L. monocytogenes-induced actin assembly requires the actA gene product, a surface protein. *Cell*, *68*, 521–531.

Lam, G. Y., Cemma, M., Muise, A. M., Higgins, D. E., & Brumell, J. H. (2013). Host and bacterial factors that regulate LC3 recruitment to Listeria

monocytogenes during the early stages of macrophage infection. *Autophagy*, *9*, 985–995.

Lamason, R. L., & Welch, M. D. (2017). Actin-based motility and cell-to-cell spread of bacterial pathogens. *Current Opinion in Microbiology*, *35*, 48–57.

Lauer, P., Chow, M. Y., Loessner, M. J., Portnoy, D. A., & Calendar, R. (2002). Construction, characterization, and use of two Listeria monocytogenes site-specific phage integration vectors. *Journal of Bacteriology*, *184*, 4177–4186.

Lauer, P., Theriot, J. A., Skoble, J., Welch, M. D., & Portnoy, D. A. (2001). Systematic mutational analysis of the amino-terminal domain of the Listeria monocytogenes ActA protein reveals novel functions in actin-based motility. *Molecular Microbiology*, *42*, 1163–1177.

Manzanillo, P. S., Ayres, J. S., Watson, R. O., Collins, A. C., Souza, G., Rae, C. S., … Cox, J. S. (2013). The ubiquitin ligase parkin mediates resistance to intracellular pathogens. *Nature*, *501*, 512–516.

Martinez, J., Malireddi, R. K., Lu, Q., Cunha, L. D., Pelletier, S., Gingras, S., … Green, D. R. (2015). Molecular characterization of LC3-associated phagocytosis reveals distinct roles for Rubicon, NOX2 and autophagy proteins. *Nature Cell Biology*, *17*, 893–906.

Meyer-Morse, N., Robbins, J. R., Rae, C. S., Mochegova, S. N., Swanson, M. S., Zhao, Z., … Portnoy, D. (2010). Listeriolysin O is necessary and sufficient to induce autophagy during Listeria monocytogenes infection. *PLoS One*, *5*, e8610.

Mitchell, G., Chen, C., & Portnoy, D. A. (2016). Strategies used by bacteria to grow in macrophages. *Microbiology Spectrum*, *4*.

Mitchell, G., Cheng, M. I., Chen, C., Nguyen, B. N., Whiteley, A. T., Kianian, S., … Portnoy, D. A. (2018). Listeria monocytogenes triggers noncanonical autophagy upon phagocytosis, but avoids subsequent growth-restricting xenophagy. *Proceedings of the National Academy of Sciences of the United States of America*, *115*, E210–E217.

Mitchell, G., Ge, L., Huang, Q., Chen, C., Kianian, S., Roberts, M. F., … Portnoy, D. A. (2015). Avoidance of autophagy mediated by PlcA or ActA is required for Listeria monocytogenes growth in macrophages. *Infection and Immunity*, *83*, 2175–2184.

Mitchell, G., & Isberg, R. R. (2017). Innate immunity to intracellular pathogens: Balancing microbial elimination and inflammation. *Cell Host & Microbe*, *22*, 166–175.

Mostowy, S. (2013). Autophagy and bacterial clearance: A not so clear picture. *Cellular Microbiology*, *15*, 395–402.

Mostowy, S., Sancho-Shimizu, V., Hamon, M. A., Simeone, R., Brosch, R., Johansen, T., & Cossart, P. (2011). p62 and NDP52 proteins target intracytosolic Shigella and Listeria to different autophagy pathways. *The Journal of Biological Chemistry*, *286*, 26987–26995.

Mostowy, S., & Shenoy, A. R. (2015). The cytoskeleton in cell-autonomous immunity: Structural determinants of host defence. *Nature Reviews Immunology*, *15*, 559–573.

National Research Council (1996). *Guide for the care and use of laboratory animals*. Washington, DC: National Academies Press.

Niebuhr, K., Ebel, F., Frank, R., Reinhard, M., Domann, E., Carl, U. D., … Chakraborty, T. (1997). A novel proline-rich motif present in ActA of Listeria monocytogenes and cytoskeletal proteins is the ligand for the EVH1 domain, a protein module present in the Ena/VASP family. *The EMBO Journal*, *16*, 5433–5444.

Noad, J., von der Malsburg, A., Pathe, C., Michel, M. A., Komander, D., & Randow, F. (2017). LUBAC-synthesized linear ubiquitin chains restrict cytosol-invading bacteria by activating autophagy and NF-kappaB. *Nature Microbiology*, *2*, 17063.

Ogawa, M., Yoshimori, T., Suzuki, T., Sagara, H., Mizushima, N., & Sasakawa, C. (2005). Escape of intracellular Shigella from autophagy. *Science*, *307*, 727–731.

Pareja, M. E., & Colombo, M. I. (2013). Autophagic clearance of bacterial pathogens: Molecular recognition of intracellular microorganisms. *Frontiers in Cellular and Infection Microbiology*, *3*, 54.

Perrin, A. J., Jiang, X., Birmingham, C. L., So, N. S., & Brumell, J. H. (2004). Recognition of bacteria in the cytosol of Mammalian cells by the ubiquitin system. *Current Biology: CB*, *14*, 806–811.

Pillich, H., Puri, M., & Chakraborty, T. (2017). ActA of Listeria monocytogenes and its manifold activities as an important listerial virulence factor. *Current Topics in Microbiology and Immunology*, *399*, 113–132.

Pistor, S., Chakraborty, T., Niebuhr, K., Domann, E., & Wehland, J. (1994). The ActA protein of Listeria monocytogenes acts as a nucleator inducing reorganization of the actin cytoskeleton. *The EMBO Journal*, *13*, 758–763.

Pistor, S., Grobe, L., Sechi, A. S., Domann, E., Gerstel, B., Machesky, L. M., … Wehland, J. (2000). Mutations of arginine residues within the 146-KKRRK-150 motif of the ActA protein of Listeria monocytogenes abolish intracellular motility by interfering with the recruitment of the Arp2/3 complex. *Journal of Cell Science*, *113*(Pt 18), 3277–3287.

Portnoy, D. A., Auerbuch, V., & Glomski, I. J. (2002). The cell biology of Listeria monocytogenes infection: The intersection of bacterial pathogenesis and cell-mediated immunity. *The Journal of Cell Biology*, *158*, 409–414.

Poussin, M. A., & Goldfine, H. (2010). Evidence for the involvement of ActA in maturation of the Listeria monocytogenes phagosome. *Cell Research*, *20*, 109–112.

Randow, F., & Youle, R. J. (2014). Self and nonself: How autophagy targets mitochondria and bacteria. *Cell Host & Microbe*, *15*, 403–411.

Schnupf, P., & Portnoy, D. A. (2007). Listeriolysin O: A phagosome-specific lysin. *Microbes and Infection / Institut Pasteur*, *9*, 1176–1187.

Simon, R., Priefer, U., & Puhler, A. (1983). A broad host range mobilization system for in vivo genetic engineering: Transposon mutagenesis in gram negative bacteria. *Nature Biotechnology*, *1*, 784–791.

Skoble, J., Auerbuch, V., Goley, E. D., Welch, M. D., & Portnoy, D. A. (2001). Pivotal role of VASP in Arp2/3 complex-mediated actin nucleation, actin branch-formation, and Listeria monocytogenes motility. *The Journal of Cell Biology*, *155*, 89–100.

Skoble, J., Portnoy, D. A., & Welch, M. D. (2000). Three regions within ActA promote Arp2/3 complex-mediated actin nucleation and Listeria monocytogenes motility. *The Journal of Cell Biology*, *150*, 527–538.

Smith, G. A., Marquis, H., Jones, S., Johnston, N. C., Portnoy, D. A., & Goldfine, H. (1995). The two distinct phospholipases C of Listeria monocytogenes have overlapping roles in escape from a vacuole and cell-to-cell spread. *Infection and Immunity*, *63*, 4231–4237.

Smith, G. A., Theriot, J. A., & Portnoy, D. A. (1996). The tandem repeat domain in the Listeria monocytogenes ActA protein controls the rate of actin-based motility, the percentage of moving bacteria, and the localization of vasodilator-stimulated phosphoprotein and profilin. *The Journal of Cell Biology*, *135*, 647–660.

Tattoli, I., Sorbara, M. T., Yang, C., Tooze, S. A., Philpott, D. J., & Girardin, S. E. (2013). Listeria phospholipases subvert host autophagic defenses by stalling pre-autophagosomal structures. *The EMBO Journal*, *32*, 3066–3078.

Theriot, J. A., Mitchison, T. J., Tilney, L. G., & Portnoy, D. A. (1992). The rate of actin-based motility of intracellular Listeria monocytogenes equals the rate of actin polymerization. *Nature*, *357*, 257–260.

Thurston, T. L., Wandel, M. P., von Muhlinen, N., Foeglein, A., & Randow, F. (2012). Galectin 8 targets damaged vesicles for autophagy to defend cells against bacterial invasion. *Nature*, *482*, 414–418.

Tilney, L. G., & Portnoy, D. A. (1989). Actin filaments and the growth, movement, and spread of the intracellular bacterial parasite, Listeria monocytogenes. *The Journal of Cell Biology*, *109*, 1597–1608.

van Wijk, S. J. L., Fricke, F., Herhaus, L., Gupta, J., Hotte, K., Pampaloni, F., … Dikic, I. (2017). Linear ubiquitination of cytosolic Salmonella Typhimurium activates NF-kappaB and restricts bacterial proliferation. *Nature Microbiology*, *2*, 17066.

Vincent, W. J., Freisinger, C. M., Lam, P. Y., Huttenlocher, A., & Sauer, J. D. (2016). Macrophages mediate flagellin induced inflammasome activation and host defense in zebrafish. *Cellular Microbiology*, *18*, 591–604.

Watson, R. O., Manzanillo, P. S., & Cox, J. S. (2012). Extracellular M. tuberculosis DNA targets bacteria for autophagy by activating the host DNA-sensing pathway. *Cell*, *150*, 803–815.

Welch, M. D., & Way, M. (2013). Arp2/3-mediated actin-based motility: A tail of pathogen abuse. *Cell Host & Microbe*, *14*, 242–255.

Whiteley, A. T., Garelis, N. E., Peterson, B. N., Choi, P. H., Tong, L., Woodward, J. J., & Portnoy, D. A. (2017). c-di-AMP modulates Listeria monocytogenes central metabolism to regulate growth, antibiotic resistance and osmoregulation. *Molecular Microbiology*, *104*, 212–233.

Yoshikawa, Y., Ogawa, M., Hain, T., Yoshida, M., Fukumatsu, M., Kim, M., … Sasakawa, C. (2009). Listeria monocytogenes ActA-mediated escape from autophagic recognition. *Nature Cell Biology*, *11*, 1233–1240.

Zuckert, W. R., Marquis, H., & Goldfine, H. (1998). Modulation of enzymatic activity and biological function of Listeria monocytogenes broad-range phospholipase C by amino acid substitutions and by replacement with the Bacillus cereus ortholog. *Infection and Immunity*, *66*, 4823–4831.

SUPPORTING INFORMATION

Additional supporting information may be found online in the Supporting Information section at the end of the article.

How to cite this article: Cheng MI, Chen C, Engström P, Portnoy DA, Mitchell G. Actin-based motility allows *Listeria monocytogenes* to avoid autophagy in the macrophage cytosol. *Cellular Microbiology*. 2018;e12854. https://doi.org/10.1111/cmi.12854